

MHD Effects on Non-Darcy Forced Convection Boundary Layer Flow past a Permeable Wedge in a Porous Medium with Uniform Heat Flux

A. M. Rashad¹, A.Y. Bakier²

¹Department of Mathematics, Faculty of Science, South Valley University
Aswan, Egypt
am_rashad@yahoo.com

²Department of Mathematics, Faculty of Science, Assuit University
Assuit, Egypt

Received: 2008.05.21 **Revised:** 2009-01-29 **Published online:** 2009-05-26

Abstract. The steady two-dimensional laminar forced flow and heat transfer of a viscous incompressible electrically conducting and heat-generating fluid past a permeable wedge embedded in non-Darcy high-porosity ambient medium with uniform surface heat flux has been studied. The governing equations are derived using the usual boundary layer and Bossinesq approximations and accounting for the applied magnetic field, permeability of porous medium, variable porosity, inertia and heat generation effects. These equations and boundary conditions are non-dimensionalized and transformed using non-similarity transformation. The resulting non-linear partial differential equations are then solved numerically subject to the transformed boundary conditions by a finite difference method. Comparisons with previously published works are performed and the results are found to be in excellent agreement. Numerical and graphical results for the velocity and temperature profiles as well as the skin friction and Nusselt number are presented and discussed for various parametric conditions.

Keywords: forced convection, porous medium, wedge flow, uniform heat flux.

1 Introduction

Convective heat transfer from surfaces embedded in porous media has been the topic of several studies in recent years. This interest in the subject stems from various engineering applications in geothermal reservoirs, petroleum industries, transpiration cooling, storage of nuclear waste materials, separation processes in chemical industries, building thermal insulation, and solar heating systems. Early work on porous media used the Darcy law that neglects important effects such as boundary and inertia effects. Vafai and Tien [1] have reported a pioneering work on the boundary and inertia effects of porous media on convective flow and heat transfer situations. In recent years, enhanced models of porous

media have been reported. These models have been applied for simulating more generalized situations such as flow through packed and fluidized beds and liquid metal flow through dendritic structures in alloy casting (Nithiarasu et al. [2]). Some of these models deal with variable porosity effects near the boundary in which the porosity distribution exhibits a peak value there and then decays asymptotically beyond that value. The basis for these models was the early experimental work of Benenati and Brosilow [3] on void fraction distribution in packed beds. Examples of such models are reported and employed by Vafai [4], Vafai et al. [5], Poulikakos and Renken [6], and Nithiarasu et al. [2]. Other models have dealt with thermal dispersion or secondary flow effect in porous media which result from mixing and recalculation of local fluid particles through tortuous paths formed by the spherical particles in packed beds. Examples of these models have been reported by Cheng and Vortmeyer [7] and Amiri and Vafai [8].

Also, Darcy's law has been the momentum equation used in many studies of fluid flow in porous media. Because Darcy's law is of order one less than the Navier-Stokes equation, only the impermeable boundary condition at a surface can be satisfied; the no-slip boundary condition cannot. In contrast with rocks, soil, sand, and other media that do fall within this category, certain porous materials, such as foam metals and fibrous media, usually have high porosities. In these media, the boundary and inertia effects not included in Darcy's model may alter the flow and heat-transfer characteristics. It is therefore necessary to determine the conditions under which these effects are important. When the Reynolds number based on the pore size is greater than unity and there is a boundary impermeable wall, the non-Darcy effects (the inertia and boundary effects) should be included in the momentum equation. The inertia effects can be accommodated through the so-called Forchheimer's extension, while the boundary effects can be modeled, in a formalization known as Brinkman's extension, through the inclusion of a viscous shear-stress term.

On other hand, hydromagnetic flows and heat transfer in porous media have been considered extensively in recent years due to their occurrence in several engineering processes such as compact heat exchangers, metallurgy, casting, filtration of liquid metals, cooling of nuclear reactors and fusion control. Ram [9] considered hydromagnetic heat and mass transfer through a porous medium in a rotating fluid. The steady free convection flow over a vertical plate in highly porous media taking into account the convective and viscous terms in the momentum equation has been investigated by Raptis and Kofousias [10]. Takhar and Beg [11] have reported on the effects of transverse magnetic field on mixed convection flow over a vertical plate embedded in porous medium. Rees and Pop [12] examined the effect of the variable permeability on the free convection flow on a vertical surface in a porous medium. The natural convection flow over a thin vertical cylinder, which is moving with a constant velocity in a non-Darcy high-porosity ambient medium, has been studied by [13]. Takhar et al. [14] has investigated the natural convection boundary-layer flow of an absorbing and electrically-conducting fluid over a semi-infinite, ideally transparent, inclined flat plate embedded in a porous medium with variable porosity. Effects of non-uniform wall temperature or mass transfer in finite sections of an inclined plate on the MHD natural convection flow in a temperature stratified high-porosity medium have considered by Takhar et al. [15]. The natural convection flow over

a vertical heated surface in a porous medium has been studied by Mittal [16]. The non-Darcy effects on the natural convection boundary layer flow on an isothermal vertical flat plate embedded in a high-porosity medium was considered by Chen et al. [17]. Minto et al. [18], Yin [19], and Rees and Pop [20] carried out some more recent studies on this topic.

Finally, steady two-dimensional laminar forced flow and heat transfer from a wedge was considered in great detail by Lin et al. [21]. They proposed a similarity solution for an isothermal surface as well as for a uniform heat flux surface for a wide range of Prandtl numbers. Koh and Hartnett [22] studied the incompressible laminar flow over a porous wedge with suction and a variable wall temperature. Watanabe [23] investigated thermal boundary layer flow over a uniform surface temperature wedge with a transpiration velocity in forced flow. Yih [24] extended the above problem by considering the heat transfer characteristics in the forced flow over wedge subjected to a uniform wall heat flux. Hossain et al. [25] investigated also the same problem by having temperature dependent viscosity as well as thermal conductivity on the forced flow past a wedge and heat transfer of a viscous incompressible fluid with uniform surface heat flux.

The aim of the present theoretical study is to investigate the effects of porosity, permeability of the porous medium, inertia and magnetic field on the flow and heat transfer of a viscous incompressible electrically conducting and heat-generating fluid past a permeable wedge embedded in fluid-saturated high-porosity ambient medium, using the extension of the Darcy-Forchheimer-Brinkman model, in the presence the magnetic field and internal heat generation effects. The surface of the wedge is maintained uniform surface heat flux and is permeable to allow for possible fluid wall suction. The resulting non-linear partial differential equations are solved numerically by a finite difference method. The results with uniform porosity and in the absence of permeability, inertia, magnetic field and heat generation effects are compared with those Yih [24] and Hossain et al. [25] with uniform both of the dynamical viscosity and thermal conductivity. Comparisons with previously published works were performed and results were found to be in a good agreement for different values of Pr and pressure gradient parameter m . Numerical and graphical results for the velocity and temperature profiles as well as the skin friction and Nusselt number are presented and discussed for various parametric conditions. Note that, numerical and graphical results for a fluid having the value of $Pr = 0.7$ that is appropriate for helium (400 °F), hydrogen (near about 370 °F) and oxygen (near about 10 °F) and $m = 1/3$.

2 Problem formulation

The physical model of the problem and the coordinates system are given in Fig. 1. Consider the steady two-dimensional laminar forced flow of an incompressible viscous electrically conducting and heat-generating fluid past a permeable wedge with uniform heat flux. The wedge is embedded in a non-Darcy high-porosity medium. A uniform magnetic field is applied in the transverse direction y normal to the wedge. According to assumption that Bossinesq approximation is valid and using the extension of the Darcy-

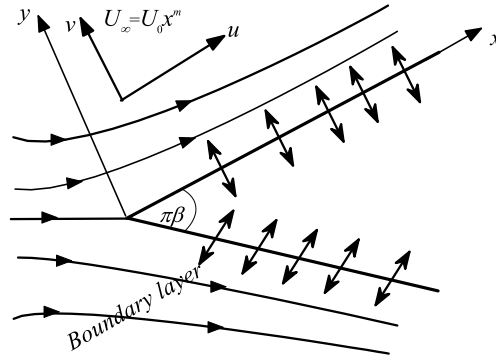


Fig. 1. The flow configuration and the coordinate system.

Forchheimer-Brinkman model, the equation of continuity, momentum and energy of the two dimensional under boundary layer form of the forced flow of the fluid past a wedge in a non-Darcy high-porosity medium modified to account for the presence magnetic field and heat generation effects can be expressed as [23–25]:

$$\frac{\partial u}{\partial x} + \frac{\partial v}{\partial y} = 0, \tag{1}$$

$$\begin{aligned} \varepsilon^{-2} \left(u \frac{\partial u}{\partial x} + v \frac{\partial u}{\partial y} \right) &= U_\infty \frac{dU_\infty}{dx} + \frac{\nu}{\varepsilon} \frac{\partial^2 u}{\partial y^2} + \frac{\nu}{K^*} (U_\infty - u) \\ &+ C^* (U_\infty^2 - u^2) + \frac{\sigma B^2}{\rho} (U_\infty - u), \end{aligned} \tag{2}$$

$$u \frac{\partial T}{\partial x} + v \frac{\partial T}{\partial y} = \alpha \frac{\partial^2 T}{\partial y^2} + \frac{Q_0(x)}{\rho C_p} (T - T_\infty). \tag{3}$$

The boundary conditions are the no-slip at the surface and the ambient condition far away from the surface and these are expressed as:

$$\begin{aligned} u = 0, \quad v = V_w, \quad -k \left(\frac{\partial T}{\partial y} \right)_{y=0} &= q_w \quad \text{at } y = 0, \\ u \rightarrow U_\infty = U_0 x^m, \quad T \rightarrow T_\infty &\quad \text{as } y \rightarrow \infty. \end{aligned} \tag{4}$$

Here u, v are fluid velocity components in the x - and y -direction, respectively, T is the temperature of the fluid in the boundary layer region, V_w is the transpiration velocity, which is positive for injection or blowing and negative for suction or withdrawal of fluid through the wedge surface, $U_\infty(x)$ being the free stream velocity, U_0 is the constant velocity of the potential flow outside the boundary layer, $m = \beta/(2 - \beta)$ is the pressure gradient parameter, β is the Hartee pressure gradient parameter which is related to the total angle of the wedge, Ω , by $\Omega = \pi\beta$. ν, ρ, σ, C_p are the kinematic viscosity,

the density of the fluid and electrical conductivity and specific heat, respectively; ε is the porosity; K is the permeability of porous medium; C^* is the inertia coefficient; $B, T_\infty, Q_0(x)$ are the magnetic induction, ambient temperature and volumetric rate of heat generation/absorption coefficient, respectively; α is thermal diffusivity; q_w is the surface heat flux, k the thermal conductivity; and subscripts w and ∞ denote conditions at the wall and in the ambient fluid, respectively. It should be mentioned here that the wedge and porous medium are both in local equilibrium. In addition, positive values of Q_0 indicate heat generation (source) and negative values of Q_0 correspond to heat absorption (sink).

It is convenient to reduce the number of equations from three to two as well as to transform them to dimensionless form. This can be done by applying the following transformations

$$\begin{aligned}\xi &= \frac{-V_x}{\nu} \sqrt{\frac{2}{1+m}} Re_x^{-1/2}, \quad \eta = \sqrt{\frac{1+m}{2}} Re_x^{1/2}, \quad u = \frac{\partial \psi}{\partial y}, \quad v = -\frac{\partial \psi}{\partial x}, \\ \psi(x, y) &= \nu \sqrt{\frac{2}{1+m}} Re_x^{1/2} f(\xi, \eta), \quad \theta(\xi, \eta) = \frac{T - T_\infty}{(q_w/k) Re_x^{1/2}}, \\ Re_x &= U_\infty x / \nu, \quad M = Ha_x^2 / Re_x, \quad Ha_x^2 = \sigma B^2 x^2 / \mu, \\ K &= K^* Re_x / x^2, \quad C = (C^* \nu / U_\infty) Re_x, \quad Pr = \nu / \alpha, \quad Q = Q_0(x) x / Re_x \rho C_p, \quad (5)\end{aligned}$$

to equations (1)–(3) and we find that (1) is identically satisfied and (2) and (3) reduce to,

$$\begin{aligned}\varepsilon^{-1} f''' + \frac{2m}{1+m} + \varepsilon^{-2} \left(f f'' - \frac{2m}{1+m} f'^2 \right) + \frac{2}{1+m} (M + K^{-1})(1 - f') \\ + \frac{2m}{1+m} C (1 - f'^2) = \varepsilon^{-2} \frac{1-m}{1+m} \xi \left(f' \frac{\partial f'}{\partial \xi} - f'' \frac{\partial f}{\partial \xi} \right), \quad (6)\end{aligned}$$

$$\frac{1}{Pr} \theta'' + f \theta' + \frac{2}{1+m} Q \theta - \frac{1-m}{1+m} f' \theta = \frac{1-m}{1+m} \xi \left(f' \frac{\partial \theta}{\partial \xi} - \theta' \frac{\partial f}{\partial \xi} \right). \quad (7)$$

The boundary conditions as (4) can be expressed as

$$f(\xi, 0) = f'(\xi, 0) = 0, \quad \theta'(\xi, 0) = -1, \quad f'(\xi, \infty) = 1, \quad \theta(\xi, \infty) = 0. \quad (8)$$

In addition, the velocity components are

$$u = U_\infty f', \quad v = -\frac{\nu}{x} \sqrt{\frac{2}{1+m}} Re_x^{1/2} \left[\frac{1+m}{2} f + \frac{1-m}{2} \left(\xi \frac{\partial f}{\partial \xi} - \eta f' \right) \right]. \quad (9)$$

Here ξ, η are the transformed coordinates, where ξ is the suction parameter and η is the pseudo-similarity variable; ψ and f are the dimensional and dimensionless stream functions, respectively; f' is the dimensionless velocity in the axial direction; θ is the dimensionless temperature; Pr, Re_x are the Prandtl number and local Reynolds number, respectively. K is the dimensionless permeability parameter; C is the dimensionless inertia coefficient expressing the relative importance of the inertia effect; M is the magnetic

parameter. In the foregoing equations, the primes denote the differentiation with respect to η . For surface blowing, $V_w > 0$ and hence $\xi < 0$. On the other hand, for surface suction, $V_w < 0$ and hence $\xi > 0$.

It may be remarked that equations governing the forced flow over the wedge can be reduced to those of Watanabe [23], Yih [24] and Hossain et al. [25] for $M = Q = 0$ (without magnetic and heat generation effects), $\varepsilon = 1$ (uniform medium), $K^{-1} = C = 0$ (in the absence of the permeability and inertia parameters).

The quantities of physical interest are the local Nusselt number and the local skin friction coefficient C_{fx} and these are expressed as

$$C_{fx} = \frac{\tau_w x}{(1/2)\rho U_\infty^2} \quad \text{and} \quad Nu_x = \frac{q_w x}{k(T - T_\infty)}, \quad (10)$$

where τ_w is the shear stress at the surface

$$\tau_w = \mu \left(\frac{\partial u}{\partial y} \right)_{y=0}. \quad (11)$$

Now incorporating the transformations given in (5) in the foregoing relations for the local Nusselt number Nu_x and the local skin friction coefficient C_{fx} hold:

$$\frac{1}{\sqrt{2}(1+m)} C_{fx} Re_x^{1/2} = f''(\xi, 0), \quad (12)$$

and

$$\sqrt{\frac{2}{1+m}} \frac{Nu_x}{Re_x^{1/2}} = \theta(\xi, 0). \quad (13)$$

3 Numerical scheme

The numerical scheme to solve equations (6) and (7) adopted here is based on a combination of the following concepts:

- (a) The boundary conditions for $\eta = \infty$ are replaced by $f'(\xi, \eta_{max}) = 1$, $\theta(\xi, \eta_{max}) = 0$, where η_{max} is a sufficiently large value of η at which the boundary conditions (8) for velocity is satisfied. We have set $\eta_{max} = 6.0$ in the present work.
- (b) The two-dimensional domain of interest (ξ, η) is discretized with an equispaced mesh in the ξ -direction and another equispaced mesh in the η -direction.
- (c) The partial derivatives with respect to ξ and η are all evaluated by the central difference approximations.
- (d) Two iteration loops based on the successive substitution are used because of the nonlinearity of the equations.

- (e) In each inner iteration loop, the value of ξ is fixed while each of equations (6) and (7) is solved as a linear second order boundary value problem of ODE on the η domain. The inner iteration is continued until the nonlinear solution converges for the fixed value of ξ .
- (f) In the outer iteration loop, the value of ξ is advanced. The derivatives with respect to ξ are updated after every outer iteration step.

In the inner iteration step, the finite difference approximation for equations (6) and (7) is solved as a boundary value problem. The numerical results are affected by the number of mesh points in both directions. To obtain accurate results, a mesh sensitivity study was performed. After some trials, in the η -direction 190 mesh points were chosen whereas in the ξ -direction 41 mesh points were used. The tolerance for convergence was 10^{-6} . Increasing the mesh points to a larger value led to identical results.

4 Results and discussion

Numerical solutions for the governing equations (6) and (7) under conditions (8) were solved numerically by a finite difference method. In order to validate our results, we have compared the local Nusselt number $Nu_x/Re_x^{1/2}$ for $M = Q = 0$ (without magnetic and heat generation effects), $\varepsilon = 1$ (uniform medium), $K^{-1} = C = 0$ (in the absence of the permeability and inertia parameters) and $\xi = 0$ (an impermeable wedge flow), with various values of m, Pr with theoretical results of Yih [24] and Hossain et al. [25]. The results are found to be in good agreement and the comparison is presented in Table 1. Here we have found that the value of local Nusselt number increases whenever the value of the pressure gradient parameter m increases at a given value of Pr . We also observe that if Pr decreases, then there is a corresponding decrease in the value of local Nusselt number for fixed value of m means the boundary layer thickness increasing with the increase of Pr .

The effects of porosity parameter ε , inertia parameter C , dimensionless permeability K , magnetic parameter M and heat source/sink parameter Q on the skin friction coefficient and Nusselt number ($C_{fx}Re_x^{1/2}/(\sqrt{2}(1+m)), Nu_x/Re_x^{1/2}$) are shown in Tables 2, 3, respectively, when $Pr = 0.72$ and $m = 1/3$. From these tables, we can observe that both skin friction coefficient and Nusselt number increases with the increase the values of M, Q, C, ε , but decreases with the increase of K . This in turn, produces increases in this due in fact that the velocity gradient increases with the increase M, Q, C, ε , or decreases with the increase of K , but the opposite to temperature gradient. However, Nusselt number is found to be weakly dependent on M, K , while the permeability and magnetic parameters strongly affect the skin friction. On other hand, the inertia C , porosity ε , heat source/sink Q parameters are found to have significant effect on both skin friction coefficient and Nusselt number. Also, as mentioned before, Q has no effect on the fluid flow field, therefore, it has no effect on the skin-friction coefficient, that is because equations (6) and (7) are uncoupled equations.

Table 1. Comparison of $Nu_x/Re_x^{1/2}$ to previously published data at $\varepsilon = 1$, $\xi = 0$, $K^{-1} = C = 0$ and $M = Q = 0$ for different values Pr and m

Pr	m	Yih [24]	Hossain et al. [25]	Present
0.1	0.0	0.20063	0.2006	0.20064
	1/3	0.21947	0.2193	0.21949
	1.0	0.21950	0.2195	0.21953
1.0	0.0	0.45896	0.4589	0.45897
	1/3	0.54197	0.5419	0.54198
	1.0	0.57046	0.5704	0.57047
10.0	0.0	0.99786	0.9978	0.99789
	1/3	1.23177	1.2317	1.23178
	1.0	1.33879	1.3387	1.33880

Table 2. Values of the skin friction coefficient and Nusselt number $C_{fx}Re_x^{1/2}/(\sqrt{2}(1+m))$, $Nu_x/Re_x^{1/2}$ for different ε , ξ and Q at $K = 0.75$, $C = 1.0$ and $M = 1.0$

ε	Q	$C_{fx}Re_x^{1/2}/(\sqrt{2}(1+m))$		$Nu_x/Re_x^{1/2}$	
		$\varepsilon = 0.4$	$\varepsilon = 0.9$	$\varepsilon = 0.4$	$\varepsilon = 0.9$
0.0	-0.5	1.50266	2.38056	0.91553	0.96649
	0.0	1.50266	2.38056	0.62247	0.69348
	0.5	1.50266	2.38056	0.21067	0.32726
1.0	-0.5	3.12586	3.32738	1.54677	1.51279
	0.0	3.12586	3.32738	1.2615	1.21184
	0.5	3.12586	3.32738	0.86483	0.77993
2.0	-0.5	4.58968	4.37812	2.45339	2.33035
	0.0	4.58968	4.37812	2.25723	2.09899
	0.5	4.58968	4.37812	2.02976	1.81347

Table 3. Values of the skin friction coefficient and Nusselt number $C_{fx}Re_x^{1/2}/(\sqrt{2}(1+m))$, $Nu_x/Re_x^{1/2}$ for different K , C and M at $\varepsilon = 0.4$, $\zeta = 0.5$ and $Q = 0.4$

C	K	$C_{fx}Re_x^{1/2}/(\sqrt{2}(1+m))$		$Nu_x/Re_x^{1/2}$	
		$M = 1.0$	$M = 2.0$	$M = 1.0$	$M = 2.0$
1.0	0.25	2.84385	3.00901	0.39465	0.40208
	0.5	2.46079	2.66253	0.37827	0.38666
	1.0	2.23278	2.46079	0.36991	0.37827
5.0	0.25	3.64036	3.75365	0.43610	0.44023
	0.5	3.39622	3.52152	0.42680	0.43164
	1.0	3.26331	3.39622	0.42155	0.4268
10	0.25	4.34705	4.43495	0.46441	0.46676
	0.5	4.16374	4.25672	0.4593	0.46193
	1.0	4.06786	4.16374	0.45653	0.4593

Figs. 2(a), 2(b) represents the effect of magnetic parameter M on the skin friction coefficient and Nusselt number ($C_{fx} Re_x^{1/2} / (\sqrt{2}(1+m))$, $Nu_x / Re_x^{1/2}$), respectively, for $Pr = 0.7$, $m = 1/3$, $C = 1.0$, $Q = 0.5$, $K = 0.75$, $\varepsilon = 0.5$, in the range $0 \leq \xi \leq 1$. Both the skin friction coefficient and Nusselt number increases with increasing M and ξ . Consequently the momentum and thermal boundary layers are reduced. This results in higher the skin friction coefficient and Nusselt number for increasing M , whereas there is strongly affect on both the skin friction and Nusselt number for increasing ξ .

The effect of the dimensionless permeability K on velocity and temperature profiles (u/U_∞ , $\theta(\xi, \eta)$) at $Pr = 0.7$, $m = 1/3$ is shown in Figs. 3(a), 3(b), respectively. It can be observed that the velocity reduces as K increases, while temperature enhances as K increases which imply that the resistance of the medium decreases. This is due to the increased restriction resulting from decreasing the porosity of porous medium.

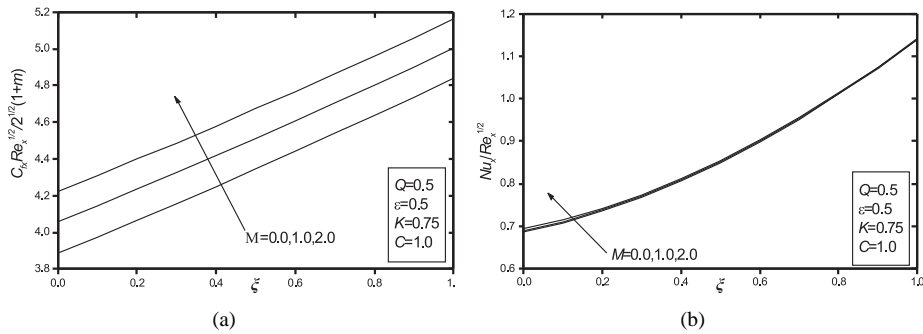


Fig. 2. Effect of M on (a) the skin friction coefficient and (b) Nusselt number, respectively.

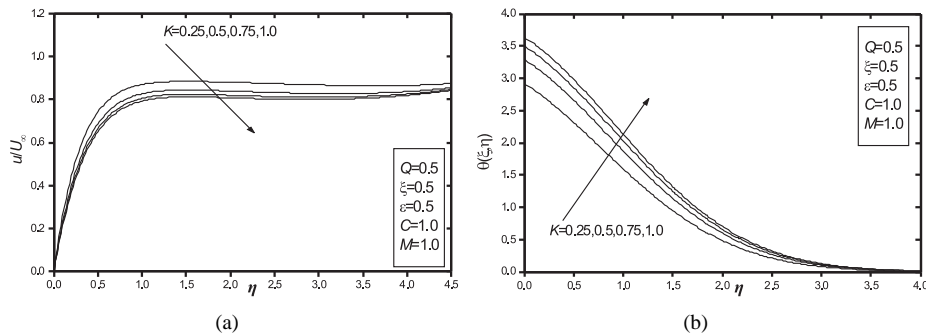


Fig. 3. Effect of K on the on (a) velocity and (b) temperature profiles, respectively.

The effect of inertia parameter C on velocity and temperature profiles (u/U_∞ , $\theta(\xi, \eta)$) at $Pr = 0.7$, $m = 1/3$ is shown in Figs. 4(a), 4(b). The decrease in inertia parameter implies more resistance to the flow which results in decrease in

the momentum boundary layer and hence in thermal boundary layer. Consequently the velocity increases and temperature decreases as C increases.

The effect of porosity parameter ε on velocity and temperature profiles (u/U_∞ , $\theta(\xi, \eta)$) at $Pr = 0.7$, $m = 1/3$ is shown in Figs. 5(a), 5(b), respectively. Since $\varepsilon = 1$ corresponds to uniform medium, decreasing ε implies less resistance is offered by the medium. Consequently the velocity increases as increases, but temperature reduces.

The effect of magnetic parameter M on velocity and temperature profiles (u/U_∞ , $\theta(\xi, \eta)$) at $Pr = 0.7$, $m = 1/3$ is shown in Figs. 6(a), 6(b), respectively. It is clear that due to an increase in values of M there is an increasing in the velocity because the unretarding effect on the magnetic force. Therefore, the momentum boundary layer thickness becomes smaller, and separation of the boundary layer will occur later. Also, we observe that the temperature profile decreases when the magnetic parameter M increases. This means that the magnetic filed works to decrease the values of temperature in the flow filed and then increases the gradient at the wall and decreases thickness of the thermal boundary layer.

The effects of heat source/sink parameter Q and the suction parameter ξ on the temperature profile (u/U_∞ , $\theta(\xi, \eta)$) at $Pr = 0.7$, $m = 1/3$ is shown in Fig. 7. It is

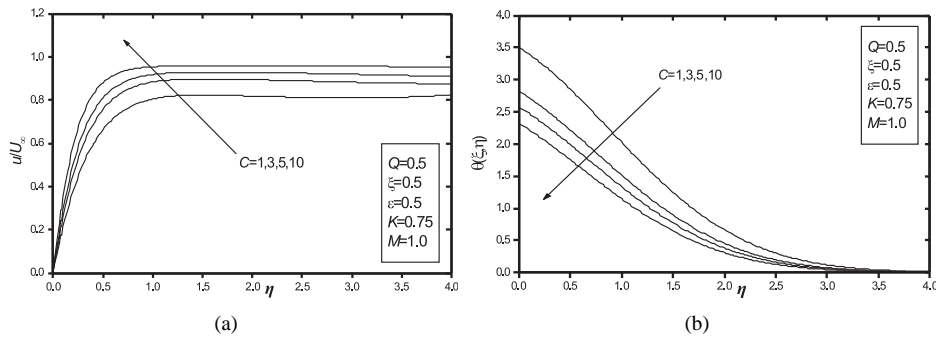


Fig. 4. Effect of C on (a) the velocity and (b) temperature profiles, respectively.

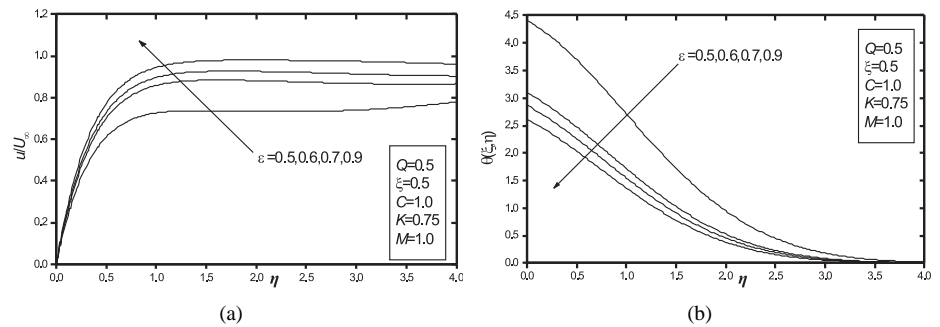


Fig. 5. Effect of ξ on (a) the velocity and (b) temperature profiles, respectively.

found that the temperature profile increases as heat source/sink parameter Q increases, but the opposite with the suction parameter ξ , therefore, the thermal boundary layer thickness becomes small for the increase of the suction parameter, while, it becomes large for the decrease of heat source/sink parameter. This is expected since heat generation ($Q > 0$) causes the thermal boundary layer to become thicker and the temperature of the fluid to increase, whereas the opposite effect with heat absorption ($Q < 0$), reducing temperature of the fluid and the thermal buoyancy effect. In addition, heat generation/absorption coefficient unaffected on the velocity flow, for the same cause mentioned above. Also, imposition of fluid suction $\xi > 0$ at a surface reduces the region of viscous domination close to the wall, which causes decreasing in the fluid's temperature profile.

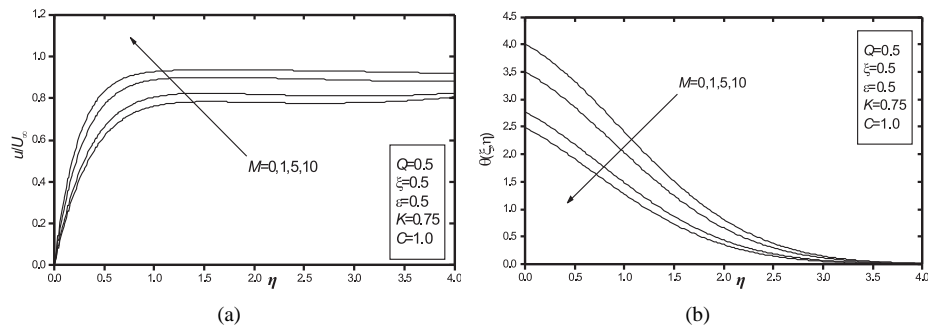


Fig. 6. Effect of M on (a) the velocity and (b) temperature profiles, respectively.

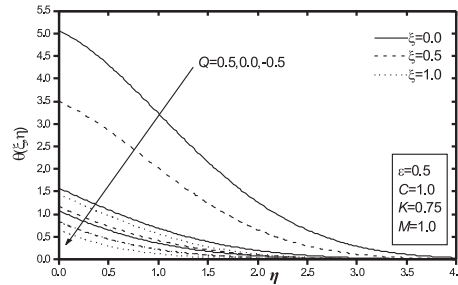


Fig. 7. Effect of Q on the temperature profiles.

5 Conclusions

The steady two-dimensional laminar forced flow of an incompressible viscous electrically conducting and heat-generating fluid past an impermeable wedge at uniform heat flux embedded in a non-Darcy high-porosity medium has been studied numerically. The governing equations are derived using the usual boundary layer and Bossinesq approximations and accounting for the applied magnetic field, permeability of porous medium,

variable porosity, inertia and heat generation effects. These equations are transformed using non-similarity transformation and then solved numerically by a finite difference method. Numerical and graphical results for the velocity and temperature profiles as well as the skin friction and Nusselt number are presented and discussed for various parametric conditions. It was found that the Nusselt number be weakly dependent on the permeability, magnetic parameters, whereas there are strongly affect the skin friction. On other hand, the Nusselt number and the skin friction are significantly affected by the inertia, porosity, suction and heat generation/absorption parameters.

Acknowledgments

The authors are grateful to the reviewers for their encouraging comments and constructive suggestions to improve the manuscript.

References

1. K. Vafai, C.L. Tien, Boundary and inertia effects on flow and heat transfer in porous media, *Int. J. Heat Mass Transfer*, **24**, pp. 195–203, 1981.
2. P. Nithiarasu, K.N. Seetharamu, T. Sundararajan, Natural convective, Heat transfer in a fluid saturated variable porosity medium, *Int. J. Heat Mass Transfer*, **40**, pp. 3955–3967, 1997.
3. R.F. Benenati, C.B. Brosilow, Void fraction distribution in packed Beds, *AIChE J.*, **8**, pp. 359–361, 1962.
4. K. Vafai, Convective flow and heat transfer in variable porosity media, *J. Fluid Mechanics*, **147**, pp. 233–259, 1984.
5. K. Vafai, R.L. Alkire, C.L. Tien, An experimental investigation of heat transfer in variable porosity media, *ASME J. Heat Transfer*, **107**, pp. 642–647, 1985.
6. D. Poulikakos, K. Renken, Forced convection in a channel filled with porous medium, including the effects of flow inertia, variable porosity, And Brinkman friction, *ASME J. Heat Transfer*, **109**, pp. 880–888, 1987.
7. P. Cheng, D. Vortmeyer, Transverse thermal dispersion and wall channeling in a packed bed with forced convective flow, *Chem. Eng. Sci.*, **43**, pp. 2523–2532, 1988.
8. A. Amiri, K. Vafai, Analysis of dispersion effects and non-thermal equilibrium, non-Darcian, variable porosity incompressible flow through porous media, *Int. J. Heat Mass Transfer*, **37**, pp. 936–954, 1994.
9. P.C. Ram, Heat and mass transfer on MHD heat generating flow through a porous medium in a rotating fluid, *Astrophys. Space Sci.*, **172**, pp. 273–277, 1989.
10. A. Raptis, N. Kafousias, Heat transfer in flow through a porous medium bounded by an infinite vertical plate under the action of a magnetic field, *Int. J. Energy Research*, **6**, pp. 97–100, 1982.
11. H.S. Takhar, O.A. Bèg, Effects of transverse magnetic field, Prandtl number and Reynolds number on non-Darcy mixed convective flow of an incompressible viscous fluid past a porous vertical flat plate in a saturated porous medium, *Int. J. Energy Research*, **21**, pp. 87–100, 1997.

12. D. A. S. Rees, I. Pop, Vertical free convection in a porous medium with variable permeability effect, *Int. J. Eng. Sci.*, **38**, pp. 2565–2572, 2000.
13. H. S. Takhar, A. J. Chamkha, G. Nath, Natural convection on a thin vertical cylinder moving in a high-porosity ambient medium, *Int. J. of Eng. Sci.*, **41**, pp. 1935–1950, 2003.
14. H. S. Takhar, A. J. Chamkha, G. Nath, Natural convection on a vertical cylinder embedded in a thermally stratified high-porosity medium, *Int. J. Therm. Sci.*, **41**, pp. 83–93, 2002.
15. H. S. Takhar, A. J. Chamkha, G. Nath, Effects of non-uniform wall temperature or mass transfer in finite sections of an inclined plate on the MHD natural convection flow in a temperature stratified high-porosity medium, *Int. J. of Therm. Sci.*, **42**, pp. 829–836, 2003.
16. M. Kaviany, M. Mittal, Natural convection heat transfer from a vertical plate to high permeability porous media: an experiment and an approximate solution, *Int. J. Heat Mass Transfer*, **30**, pp. 967–977, 1987.
17. Chen, C.I. Hung, H.C. Horng, Transient natural convection on a vertical flat plate embedded in a high porosity medium, *ASME J. Energy Res. Tech.*, **109**, pp. 112–118, 1987.
18. B. J. Minto, D. B. Ingham, I. Pop, Free convection driven by an exothermic reaction on a vertical surface embedded in porous media, *Int. J. Heat Mass Transfer*, **41**, pp. 11–24, 1998.
19. K. A. Yin, Uniform transpiration effect on the combined heat and mass transfer by natural convection over a cone in saturated porous media: Uniform temperature/concentration or heat/mass flux, *Int. J. Heat Mass Transfer*, **42**, pp. 3533–3537, 1999.
20. D. A. S. Rees, I. Pop, Vertical free convection in a porous medium with variable permeability effect, *Int. J. Eng. Sci.*, **38**, pp. 2565–2572, 2000.
21. H. T. Lin, L. K. Lin, Similarity solutions for laminar forced convection heat transfer from wedges to fluids of any Prandtl number, *Int. J. Heat Mass Tran.*, **30**, pp. 1111–1118, 1987.
22. J. C. Y. Koh, J. P. Hartnett, Skin-friction and heat transfer for incompressible laminar flow over porous wedges with suction and variable wall temperature, *Int. J. Heat Mass Tran.*, **2**, pp. 185–198, 1961.
23. T. Watanabe, Thermal boundary layer over a wedge with uniform suction or injection in forced flow, *Acta Mechanica*, **83**, pp. 119–126, 1990.
24. K.A. Yih, Uniform suction/blowing effect on the forced convection about a wedge: uniform heat flux, *Acta Mechanica*, **128**, pp. 173–181, 1998.
25. Md. Anwar Hossain, Md. Sazzad Munir, David Andrew S. Rees, Flow of viscous incompressible fluid with temperature dependent viscosity and thermal conductivity past a permeable wedge with uniform surface heat flux, *Int. J. Therm. Sci.*, **39**, pp. 635–644, 2000.